The EMBO Journal (2012) 31, 959–971 | © 2012 European Molecular Biology Organization | All Rights Reserved 0261-4189/12
www.embojournal.org

THE EMBO JOURNAL

CPEB2–eEF2 interaction impedes HIF-1α RNA translation

Po-Jen Chen[1,2] and Yi-Shuian Huang[1,2,*]

[1]Division of Neuroscience, Institute of Biomedical Sciences, Academia Sinica, Taipei, Taiwan and [2]National Defense Medical Center, Graduate Institute of Life Sciences, Taipei, Taiwan

Translation of mRNA into protein proceeds in three phases: initiation, elongation, and termination. Regulated translation allows the prompt production of selective proteins in response to physiological needs and is often controlled by sequence-specific RNA-binding proteins that function at initiation. Whether the elongation phase of translation can be modulated individually by *trans*-acting factors to synthesize polypeptides at variable rates remains to be determined. Here, we demonstrate that the RNA-binding protein, cytoplasmic polyadenylation element binding protein (CPEB)2, interacts with the elongation factor, eEF2, to reduce eEF2/ribosome-triggered GTP hydrolysis *in vitro* and slow down peptide elongation of CPEB2-bound RNA *in vivo*. The interaction of CPEB2 with eEF2 downregulates HIF-1α RNA translation under normoxic conditions; however, when cells encounter oxidative stress, CPEB2 dissociates from HIF-1α RNA, leading to rapid synthesis of HIF-1α for hypoxic adaptation. This study delineates the molecular mechanism of CPEB2-repressed translation and presents a unique model for controlling transcript-selective translation at elongation.

The EMBO Journal (2012) **31,** 959–971. doi:10.1038/emboj.2011.448; Published online 9 December 2011
Subject Categories: RNA; proteins
Keywords: CPEB; eEF2; HIF-1; translation elongation

Introduction

Translation of mRNA into protein is coordinated by the interplay of ribosomes and general translation factors. This process is composed of the following three phases: (1) Initiation: The sequential assembly of eukaryotic initiation factors (eIFs) and the 40S ribosome at the 5′ end of RNA forms the 48S complex that scans the 5′-untranslated region (5′-UTR) until it locates the AUG start codon. Upon the release of eIFs and joining of the 60S ribosomal subunit, the translation-competent 80S ribosome is assembled at the start codon ready for the next step. (2) Elongation: The open reading frame of the mRNA is decoded by the repetitive and coordinated actions of the 80S ribosome, eukaryotic elongation factors (eEFs) and aminoacyl-charged tRNAs to synthesize a specific polypeptide chain until the entire coding sequence is translated and a stop codon is reached. (3) Termination: Translation ceases in this final stage. Once the eukaryotic releasing factors (eRFs) bind to the stop codon, they prompt release of the polypeptide chain and disassembly of the entire ribosome–mRNA complex to conclude one round of translation (Merrick and Nyborg, 2000; Mathews *et al*, 2007; Pestova *et al*, 2007). In addition to the general synthesis machinery, translation of selective mRNAs can be modulated with *cis*-regulatory sequences that often reside in the 5′- or 3′-UTR of the mRNA and/or with their cognate RNA-binding proteins. Virtually, all RNA-binding proteins identified to date mechanistically regulate translation at the initiation stage (Richter and Sonenberg, 2005; Sonenberg and Hinnebusch, 2009). In contrast, polypeptide elongation is usually modulated in a general manner through phosphorylation of eEF2 to impair its binding to GTP, thereby decreasing the rate of peptide elongation and contributing to global inhibition of protein synthesis (Carlberg *et al*, 1990; Nygard *et al*, 1991). Although polysome profiling experiments indicate that the translational regulation of several transcripts likely occurs at elongation (Olsen and Ambros, 1999; Clark *et al*, 2000; Waerner *et al*, 2006; Galban *et al*, 2008), the mechanisms underlying these observations have just begun to surface with a recent report showing that the heterogeneous nuclear ribonucleoprotein (hnRNP) E1 inhibits the release of eEF1A1 from ribosomes and stops translation elongation of its target RNAs (Hussey *et al*, 2011).

The CPEB (cytoplasmic polyadenylation element binding protein)-like proteins, CPEB2, CPEB3, and CPEB4, were identified because they showed a similar structure and sequence in the C-terminal RNA-binding regions to CPEB1 (Mendez and Richter, 2001). CPEB1 represses translation via binding to the eIF4E-binding protein, maskin, or neuroguidin, which blocks translation initiation by interfering with the assembly of eIF4E and eIF4G (Stebbins-Boaz *et al*, 1999; Jung *et al*, 2006). Although the previous studies show that CPEB2 and CPEB3 repress target RNA translation (Huang *et al*, 2006; Hagele *et al*, 2009), the molecular mechanisms accounted for this inhibition have not been revealed. In the present study, using a yeast two-hybrid screen and co-immunoprecipitation (co-IP) assays, we found that CPEB2 directly interacted with the elongation factor, eEF2, for which guanosine triphosphatase (GTPase) activity is induced upon binding to ribosomes and required for peptide translocation (Merrick and Nyborg, 2000; Hartman and Smith, 2010). Using an *in-vitro* reconstituted system (Iwasaki and Kaziro, 1979), the rate of eEF2/ribosome-activated GTP hydrolysis was diminished by CPEB2. In the tethered function assay, CPEB2 inhibited the reporter RNA translation only when binding to the RNA. Such repression persisted in eIF-independent translation (Wilson *et al*, 2000; Pestova and Hellen, 2003) and was sensitive to an agent that blocks elongation, but not initiation. Moreover, CPEB2 in which the eEF2-interacting motif had been deleted lost its repressor function; thus, CPEB2 impedes target RNA translation at elongation.

*Corresponding author. Institute of Biomedical Sciences, Academia Sinica, 128 Section 2, Academia Road, N703 Taipei 11529, Taiwan.
Tel.: +886 22652 3523; Fax: +886 22785 8594;
E-mail: yishuian@ibms.sinica.edu.tw

Received: 28 May 2011; accepted: 15 November 2011; published online: 9 December 2011

The only known target of CPEB2 is hypoxia-inducible factor-1α (HIF-1α) RNA, which encodes a transcription factor that regulates several hypoxia-inducible genes. HIF-1α is constantly synthesized, prolyl-hydroxylated and degraded in the well-oxygenated environment; however, in response to hypoxia- or chemical-induced oxidative stress, the HIF-1α level is rapidly elevated due to an increase in translation and blockade of degradation (Yee Koh *et al*, 2008; Majmundar *et al*, 2010). Several polysomal profiling studies have reported that elevated HIF-1α synthesis is concomitant with the migration of HIF-1α RNA from polysomes of light density towards polysomes of heavy density (Hui *et al*, 2006; Thomas and Johannes, 2007; Galban *et al*, 2008), suggesting that upregulated HIF-1α synthesis during hypoxia may be first contributed by increasing the translation efficiency of HIF-1α RNA that are already in the elongation phase. Despite much attention is paid to investigate HIF-1α synthesis under hypoxia, it has not been assessed whether HIF-1α RNA is subject to translational control under normoxia since HIF-1α protein is degraded and barely detectable in most cells. Here, we found that the interaction between CPEB2 and eEF2 slowed down translation of HIF-1α RNA; however, arsenite-induced oxidative stress caused the dissociation of CPEB2 from HIF-1α RNA, resulting in augmentation of HIF-1α synthesis. Taken together, our study reveals the molecular mechanism underlying CPEB2-repressed translation. Notably, the CPEB2–eEF2 interaction represents a unique example in which the peptide elongation rate from individual RNA is modulated through a 3′-UTR-bound translational repressor to control the rate-limiting step of protein synthesis at elongation.

Results

Identification and expression analysis of novel CPEB2 isoforms

A previous study using northern blotting showed that CPEB2 mRNA was expressed at high levels in the testes and brain (Theis *et al*, 2003); however, the tissue distribution of CPEB2 protein has not been examined. Because CPEB2 shares 95% sequence identity with CPEB3 and CPEB4 in the C-terminal RNA-binding domain, we used the N-terminal 261 amino acids (a.a.) of mouse CPEB2 (NP_787951, 521 a.a.) as the immunogen to generate a CPEB2-specific antibody that did not recognize other CPEB proteins (Supplementary Figure S1). This affinity-purified antibody showed that CPEB2 proteins from neurons migrated at about 100 and 135 kDa on SDS–polyacrylamide gel (PAGE), which were larger than the published mouse sequence (Figure 1A). Because the immunostained signals were diminished in CPEB2 knockdown (KD) neurons (Figure 1A), the NP_787951 clone is unlikely to contain full-length CPEB2. To identify the longer transcripts, primers designed according to the predicted rat CPEB2 sequence (XM_001060239, 724 a.a.) were used to amplify the coding region from hippocampal neuron cDNA. Two unreported alternatively spliced sequences, CPEB2a and CPEB2b, were isolated and deposited in the NCBI database, JF973322 and JF973323, respectively (Figure 1B). CPEB2a and CPEB2b, when co-expressed in Neuro-2a cells, migrated at a similar position to endogenous CPEB2 of 100 kDa on SDS–PAGE (Figure 1C). Notably, a weak signal of ∼135 kDa was also detected (Figure 1C). This 135 kDa isoform (NP_787951.2) was recently deposited to replace the original NP_787951; however, most CPEB2 from neurons and Neuro-2a cells appears to be encoded by CPEB2a and CPEB2b sequences. A comparison of the genomic organization of CPEB2a, CPEB2b, and NP_787951.2 is illustrated in Figure 1D. Because the antibody was raised against the common region of all isoforms, the tissue distribution of CPEB2 was examined by western blotting. Except in the testes where the 135-kDa isoform was abundantly expressed, the predominant forms in other tissues appear to be CPEB2a/2b (Figure 1E).

CPEB2 interacts with eEF2

To understand how CPEB2 regulates translation, the N-terminal 456 a.a. of CPEB2a was used as the bait for a yeast two-hybrid screen to identify its binding partners. The plasmid DNAs isolated from clones of positive interaction were sequenced and listed (Supplementary Table I). Among them, a clone containing a.a. 717–803 of eEF2 was identified (Figure 2A). Additional analysis delineated that the domain V of eEF2 was sufficient to bind to the N-termini of rCPEB2a, rCPEB2b, and mCPEB2 (Figure 2B), suggesting the eEF2-interacting motif is located in the common region of each isoform. The CPEB2–eEF2 association was also confirmed by IP using 293T cell lysates expressing myc–CPEB2a or myc–CPEB2b along with flag–eEF2. Both isoforms pulled down flag–eEF2 (Figure 2C). When eEF2 was divided into half, flag–eEF2N (domains I, G′, and II) and flag–eEF2C (domains III, IV, and V), only the domain V-containing C-terminus was associated with myc–CPEB2a (Figure 2D). Analysis of endogenous CPEB2–eEF2 interaction was performed using Neuro-2a cell lysates. Reciprocal IP showed that CPEB2 co-precipitated with eEF2 and vice versa. This interaction was RNA independent because it was not affected by a treatment with RNase A (Figure 2E).

CPEB2 inhibits eEF2/ribosome-activated GTP hydrolysis in vitro

When complexed with GTP, eEF2 binds to the 80S ribosome that consequently activates its GTPase activity and then catalyses the translocation of the peptidyl-tRNA, deacylated tRNA, and mRNA to allow the next codon to be translated in the decoding site of the ribosome (Merrick and Nyborg, 2000; Herbert and Proud, 2007). Since eEF2/ribosome-triggered GTP hydrolysis is a prerequisite for peptide synthesis, we examined whether this activity was affected by CPEB2. The tissue-isolated eEF2 and 80S ribosome were reconstituted *in vitro* to monitor GTP hydrolysis (Iwasaki and Kaziro, 1979). Coomassie blue staining of the purified proteins on SDS–PAGE and sucrose density gradient analysis of the 80S ribosome were performed to ensure the quality of preparations (Supplementary Figure S2A). The GTPase activity of eEF2 was upregulated about 20-fold by ribosomes (Supplementary Figure S2B), which was similar to the previous study (Iwasaki and Kaziro, 1979). The rate of eEF2/ribosome-activated GTP hydrolysis was reduced about two-fold by the presence of recombinant $(His)_6$-sumo–CPEB2a compared with the control, enhanced green fluorescent protein fused to Ms2 coat protein ($(His)_6$-sumo—EGFP–Ms2CP), an artificial RNA-binding protein that was used later in the tethered function assay (Figure 3A). CPEB2 partially, but not completely, inhibited GTP hydrolysis even after prolonged

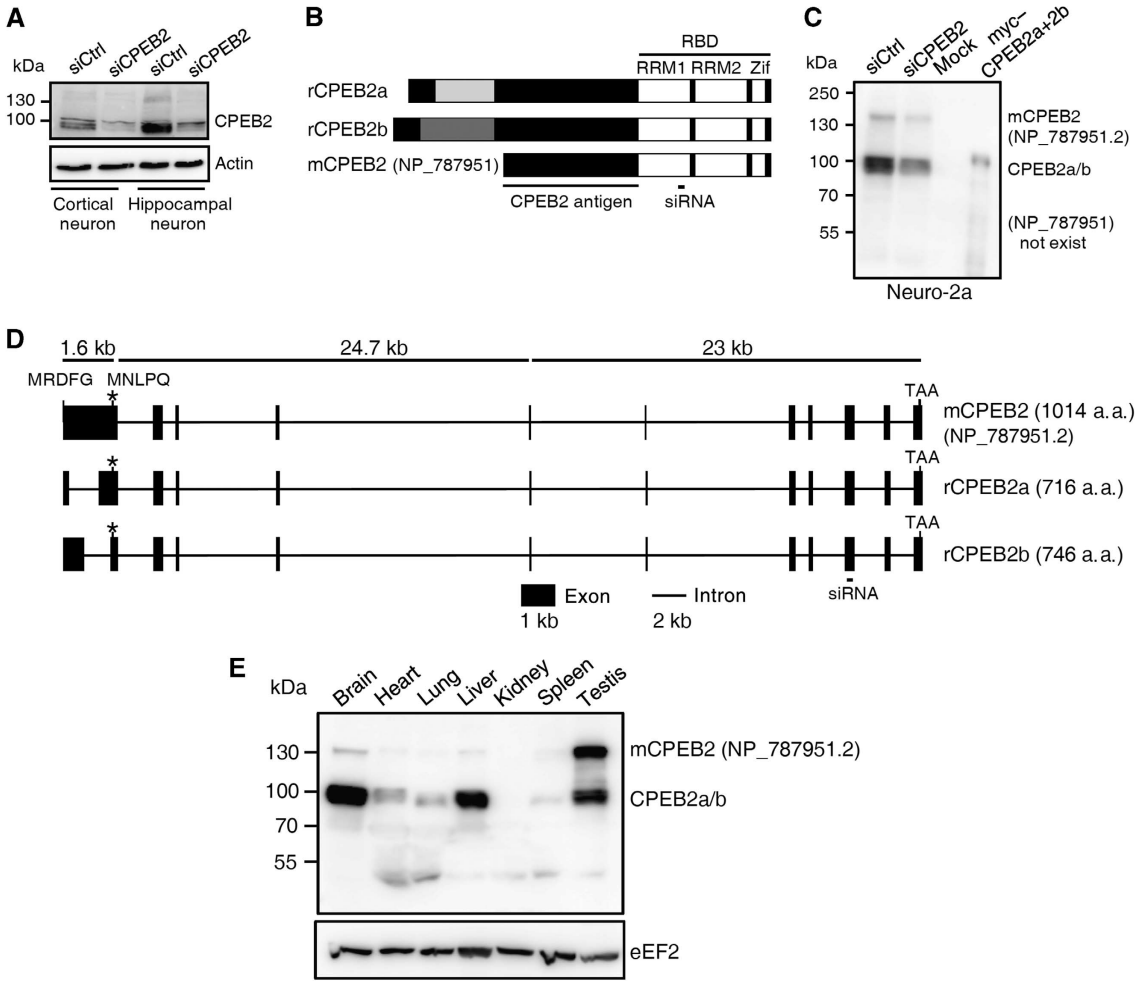

Figure 1 Identification and expression analysis of CPEB2 isoforms. (**A**) CPEB2 proteins in the control (siCtrl) and CPEB2 knockdown (siCPEB2) neurons were detected at a size of around 100 and 135 kDa (see also Supplementary Figure S1 for antibody specificity). (**B**) Two alternatively spliced forms of CPEB2, rCPEB2a, and rCPEB2b were identified from rat hippocampal neuron cDNA that encoded proteins with additional amino acids (a.a.) at the N-terminus compared with the original mouse CPEB2 clone (NP_787951). The light- and dark-gray boxes indicate unique regions in rCPEB2a and rCPEB2b, respectively. RBD, RNA-binding domain; RRM, RNA recognition motif; Zif, zinc finger. The areas used for antibody production and siRNA knockdown are underlined. (**C**) CPEB2 expression in siCtrl, siCPEB2, untransfected (mock), and overexpressed (myc–CPEB2a + 2b) Neuro-2a cells. The amount of proteins loaded from untransfected and overexpressed cells was 1/50th of that from siCtrl and siCPEB2 cells. (**D**) Genomic organization of three CPEB2 isoforms. The asterisk denotes the originally reported start codon in the NP_787951 clone. (**E**) Tissue distribution of CPEB2 in the western blot. The eEF2 signal served as a loading control. Figure source data can be found in Supplementary data.

incubation (Figure 3A) or when present at 20-fold greater concentrations than eEF2 in the reaction (Supplementary Figure S2C). The CPEB2–eEF2 interaction might preclude eEF2 docking to ribosomes or interfere with the ribosome-induced conformational change of eEF2 to affect GTP hydrolysis (Figure 3B, illustration on the left). To distinguish between the two scenarios, CPEB2 and ribosome mixtures were immunoprecipitated with CPEB2 antibody. Both 28S and 18S ribosomes co-precipitated with CPEB2 only in the presence of eEF2 as judged by the pull down of ribosomal RNAs (Figure 3B), suggesting that CPEB2 bound to ribosomal eEF2 and was likely to be polysome-associated *in vivo*. Neuro-2a cell lysates treated with or without EDTA were separated on sucrose density gradients. The gradient profiles showed that a portion of CPEB2 protein co-sedimented with polysomes. Because EDTA-induced polysome disassembly resulted in the migration of CPEB2 like the ribosomal protein S6 (RPS6) towards lighter density fractions, CPEB2 was indeed polysome-associated (Figure 3C).

CPEB2 represses target RNA translation at elongation

To determine whether CPEB2 restrained protein synthesis at elongation due to its inhibitory effect on eEF2, we used the tethered function assay (Huang and Richter, 2007). The C-terminal RNA-binding domain of CPEB2a or CPEB2b was replaced with the dimeric Ms2CP, which recognizes the unique stem-loop sequence (Ms2). EGFP–Ms2CP served as a control. The firefly luciferase reporter was appended with two Ms2 sites at the 3′-UTR in the sense (Luc) or antisense (LucR) orientation. Because Ms2CP does not bind to the complementary Ms2 sequence, the LucR reporter was used as a non-target control of Ms2CP fusions. The internal ribosomal entry site (IRES) from the cricket paralysis virus (CrPV) was added at the 5′-UTR to derive the eIF-independent reporter, CrPV-Luc (Figure 4A), because the CrPV IRES does not require any eIF for translation (Pestova and Hellen, 2003). As all reporter RNA levels were not influenced by CPEB2 (Figure 4B), any change in the firefly luciferase expression would be due to translation. Both CPEB2aN- and CPEB2bN–

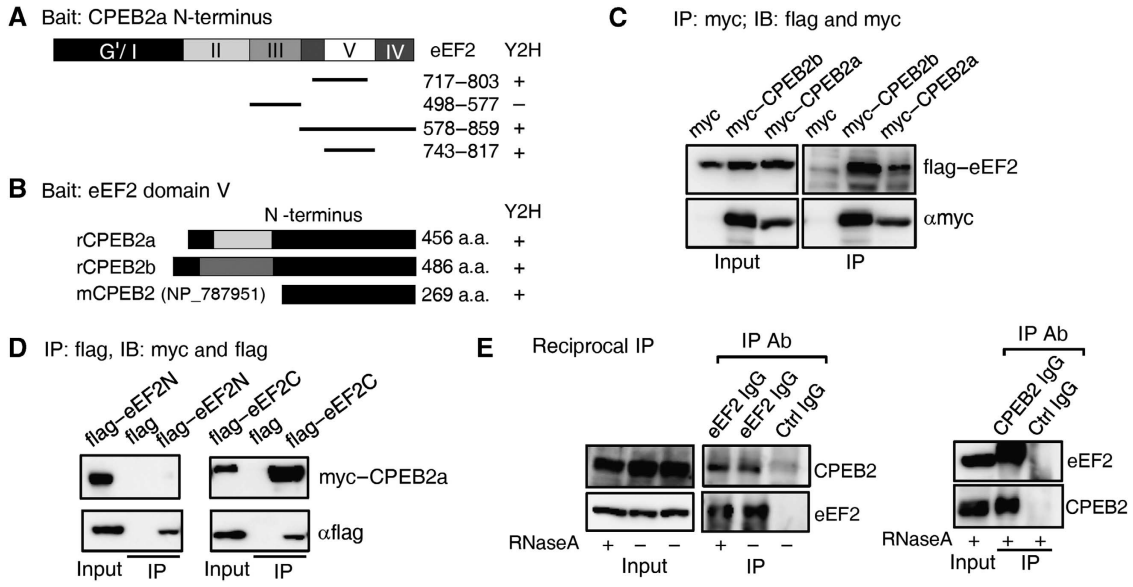

Figure 2 CPEB2 interacts with eEF2. (**A**) Using the N-terminal 456 a.a. of CPEB2a as the bait, a yeast two-hybrid (Y2H) screen identified a clone containing a.a. 717–803 of eEF2. The various truncated eEF2 mutants were tested for positive (+) or negative (−) association with the CPEB2a N-terminus. (**B**) The N-termini of CPEB2a, CPEB2b (486 a.a.), and the common region (269 a.a.) were tested for their interaction with domain V of eEF2 in the Y2H system. (**C**) Co-immunoprecipitation assay. Using 293T cells expressing flag–eEF2 along with myc–CPEB2a or myc–CPEB2b, cell lysates were precipitated with myc antibody (Ab) and immunoblotted with flag Ab. IP: immunoprecipitation, IB: immunoblotting. (**D**) Using 293T cells expressing flag–eEF2N (domains I, G′, and II) or flag–eEF2C (domains III, IV, and V) along with myc–CPEB2a, cell lysates were precipitated with flag Ab and immunoblotted with myc Ab. (**E**) Reciprocal immunoprecipitation. Neuro-2a cell lysates, with or without RNase A treatment, were precipitated with control, CPEB2, or eEF2 IgG, and immunoblotted with CPEB2 and eEF2 antibodies. Figure source data can be found in Supplementary data.

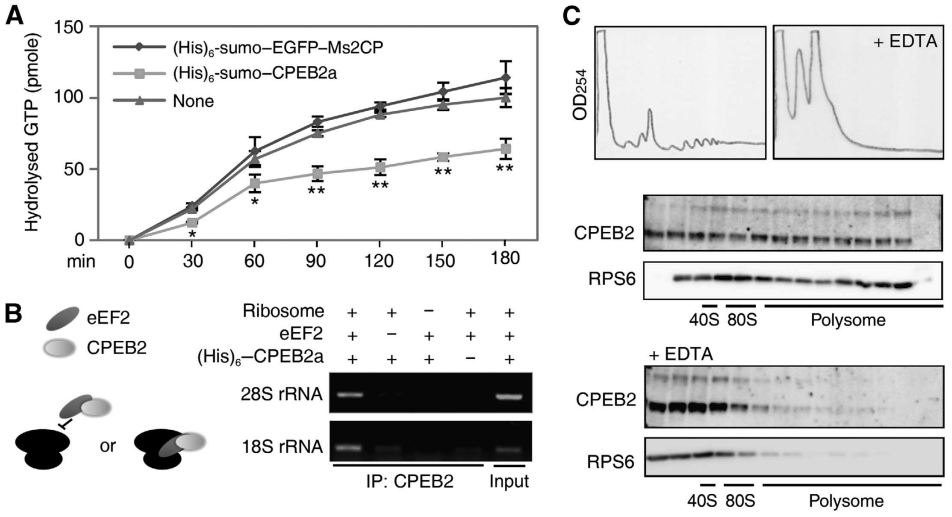

Figure 3 CPEB2 decreases eEF2/ribosome-activated GTP hydrolysis *in vitro*. (**A**) The rate of ribosome-promoted GTP hydrolysis of eEF2 was determined using purified eEF2 and the 80S ribosome in the absence (none) or presence of recombinant $(His)_6$-sumo-tagged CPEB2a or a control, EGFP–Ms2CP (see also Supplementary Figure S2). Error bars indicate s.e.m. ($n=3$). One and two asterisks denote significant differences in the amount of hydrolysed GTP at each time point between CPEB2 and EGFP–Ms2CP, with $P<0.05$ and $P<0.01$, respectively (Student's *t*-test). (**B**) CPEB2–eEF2 interaction may or may not prevent eEF2 from docking to ribosomes, as illustrated. The reactions containing different combinations of CPEB2a, 80S ribosome, and/or eEF2 were precipitated with CPEB2 Ab and analysed for 28S and 18S ribosomal RNAs (rRNAs) by reverse transcription-PCR (RT–PCR). (**C**) Polysomal distribution of CPEB2. Neuro-2a lysates were treated with or without 50 mM EDTA before sucrose density gradient centrifugation. The proteins from gradient fractions were immunoblotted with CPEB2 and ribosomal protein S6 (RPS6) antibodies. Figure source data can be found in Supplementary data.

Ms2CP repressed translation only when binding to the reporter RNAs because they exerted no effect on LucR reporter expression (Figure 4C). Moreover, CPEB2 downregulated both reporter translations including CrPV IRES-directed synthesis, suggesting this inhibition occurred at post-initiation. Next, we examined whether constrained protein synthesis with low doses of inhibitors, specifically at elongation by cycloheximide (CHX) or at initiation by 4EGI-1 (Moerke *et al*,

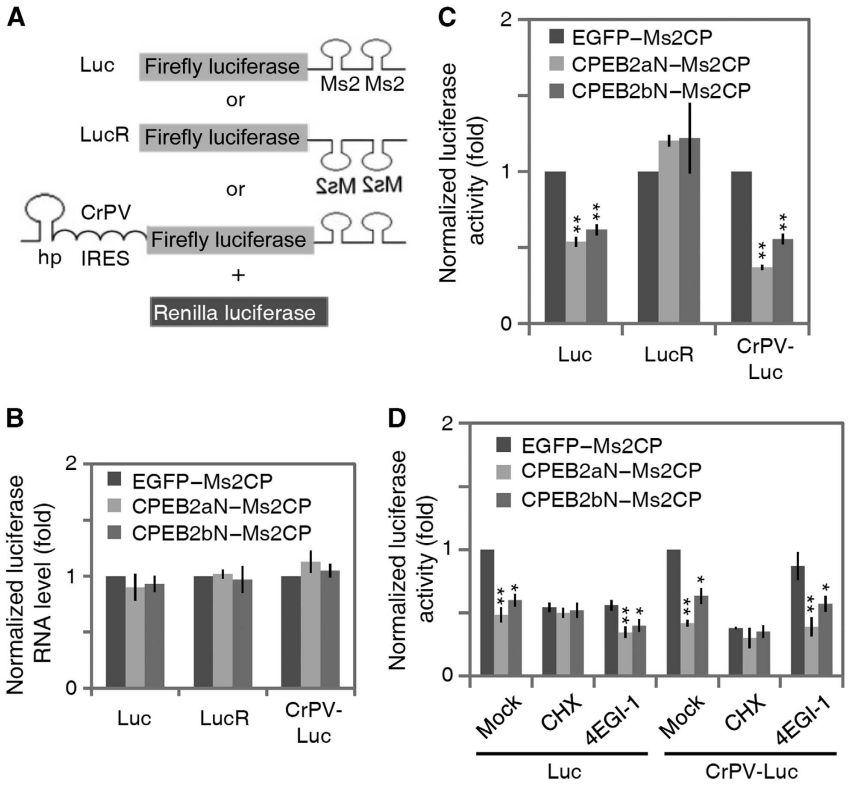

Figure 4 CPEB2 represses target RNA translation at elongation. (**A**) The reporter constructs used in the tethered function assay. The firefly luciferase was appended with 3′-UTR containing two Ms2CP-binding sites in sense (Luc) or antisense (LucR) orientation. CrPV-Luc reporter contains hairpin (hp) and internal ribosomal entry site (IRES) sequence in the 5′-UTR. *Renilla* luciferase was used to normalize variation in transfection efficiency. (**B**) The RNA-binding domain of CPEB2a (or CPEB2b) was replaced with the dimeric Ms2 coat protein (CPEB2aN–Ms2CP) and EGFP–Ms2CP was used as a control. The 293T cells transfected with the reporters and Ms2CP fusions were analysed for luciferase RNA levels by quantitative RT–PCR or (**C**) protein levels by dual luciferase assay (normalized: firefly/*Renilla*). (**D**) Similarly to (**C**), except transfected cells were treated with 2 μM cycloheximide (CHX) or 100 μM 4EGI-1 for 12 h before the assay. Error bars indicate s.e.m. (**B**, **D**) $n=3$; (**C**) $n=5$. One and two asterisks denote significant differences when compared with the EGFP–Ms2CP control, $P<0.05$ and $P<0.01$, respectively (Student's *t*-test).

2007; Lakkaraju *et al*, 2008), differentially affected CPEB2-suppressed translation. Since the synthetic molecule 4EGI-1 binds eIF4E and interrupts eIF4E–eIF4G association (Moerke *et al*, 2007), only the cap- (Luc) but not CrPV-dependent (CrPV-Luc) translation would be affected (Figure 4D). In the presence of CHX but not 4EGI-1, the inhibitory effect of CPEB2 was no longer evident (Figure 4D), supporting that CPEB2 repressed translation at elongation. Intriguingly, despite the rate-limiting step in translation for most RNAs is at initiation (Mathews *et al*, 2007), CPEB2 suppressed cap-dependent Luc RNA translation even after the initiation capacity was further downregulated by 4EGI-1 (Figure 4D). This indicates that the rate-limiting step for CPEB2-targeted translation takes place at elongation.

Translational repression activity of CPEB2 is dependent on binding to eEF2

To define the translational repression motif in CPEB2, various truncated mutants in the N-terminus of CPEB2a were fused to Ms2CP for the tethered function assay (Figure 5A). Amino-terminal truncation mutants of CPEB2a with deletions up to a.a. 187 retained most repression activity, while deletions up to a.a. 364 lost repression activity; therefore, the repression motif is located in the common region of CPEB2 isoforms. Amino acids 381–457, at the end of the CPEB2 N-terminus, were dispensable for repression activity (Figure 5B). Additional mutants with deletions within a.a. 188–364, Δ188–364, Δ188–256, and Δ257–364, showed that the entire region participated in translational repression (Figure 5B). It was recently shown that all four CPEBs shuttle between nucleocytoplasmic compartments, with longer retention time in the cytoplasm (Kan *et al*, 2010; Lin *et al*, 2010; Peng *et al*, 2010). To ensure the lack of repression was not caused by altered distribution of mutant proteins, cells transfected with those constructs were stained with myc antibody to confirm the cytoplasm-prevalent distribution (Supplementary Figure S3).

If CPEB2-downregulated translation is mediated through eEF2, the repression activity of CPEB2 mutants should correlate with their eEF2-binding ability. The 293T cell lysates containing CPEB2 mutants with or without repression activity were immunoprecipitated to determine whether they bound to eEF2. The repression-proficient mutants, Δ1–187, Δ381–457, Δ188–256, and Δ257–364, bound to eEF2; whereas the repression-defective mutants, Δ1–256, Δ1–364, and Δ188–364, did not (Figure 5C).

When using the eEF2-interacting motif (a.a. 188–364 of CPEB2) to blast the protein database, only CPEB3 and CPEB4 but not CPEB1 were identified (Supplementary Figure S4A), suggesting CPEB3 and CPEB4 may use similar mechanism to control translation. To investigate whether the other repressor, CPEB3, also inhibits translation elongation, the tethered

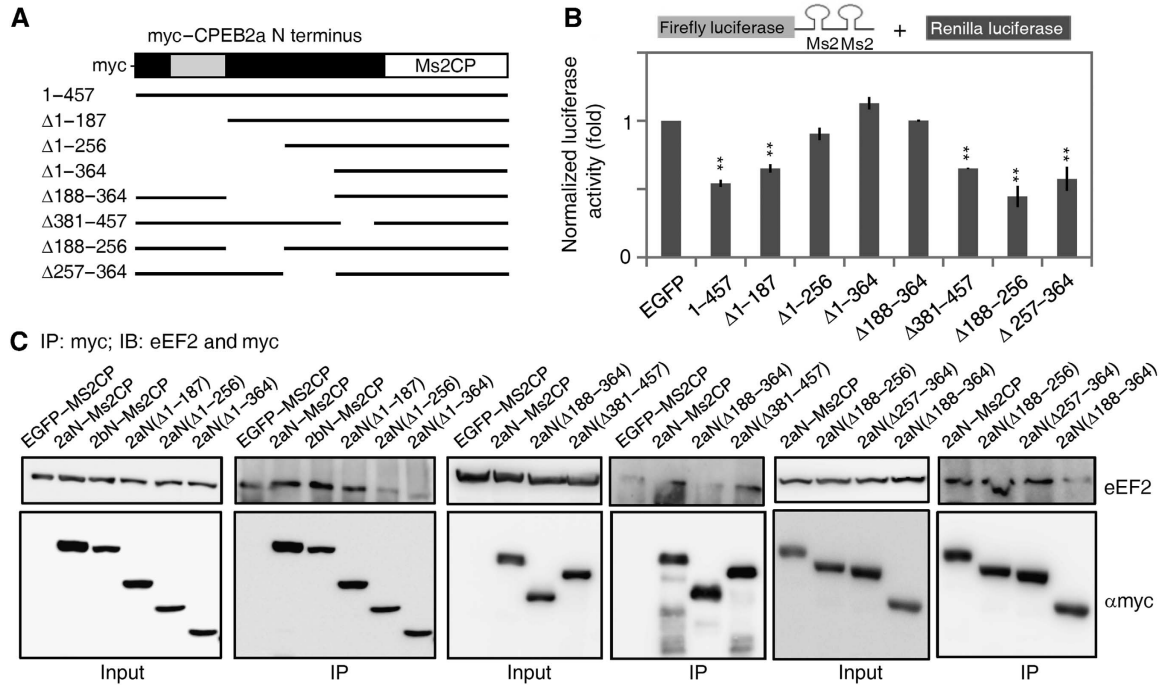

Figure 5 CPEB2-inhibited translation requires an association with eEF2. (**A**) Schemes of the various truncated myc–CPEB2aN–Ms2CP constructs (see also Supplementary Figure S3 for subcellular distribution of these mutants). (**B**) The 293T cells transfected with luciferase reporters and Ms2CP fusions were analysed by the luciferase assay (normalized: firefly/*Renilla*). Error bars indicate s.e.m. ($n=3$). Two asterisks denote a significant difference, $P<0.01$ (Student's *t*-test). (**C**) The 293T lysates expressing EGFP–Ms2CP or various myc-tagged CPEB2aN–Ms2CP mutants were immunoprecipitated with myc Ab and probed with eEF2 and myc Abs. Figure source data can be found in Supplementary data.

function assay was employed. Not only CPEB3N–Ms2CP repressed CrPV-directed translation (Supplementary Figure S4B) but also the Δ1–364 CPEB3 mutant, which lost its repression activity, was unable to associate with eEF2 (Supplementary Figure S4C–E). The deletion mutant analysis has mapped the a.a. 216–317 is essential for CPEB3 to associate with eEF2, which shares certain degree of sequence similarity with CPEB2's eEF2-interacting motif (highlighted in bold in Supplementary Figure S4A).

CPEB2 –eEF2 interaction controls the rate-limiting step of HIF-1α RNA translation at elongation

Expression of the short form of CPEB2 (521 a.a.) inhibited translation of HIF-1α RNA as well as a reporter RNA appended with HIF-1α 3′-UTR (Hagele *et al*, 2009). Several studies have found that a significant portion of HIF-1α RNA is polysome-associated under normoxia (Hui *et al*, 2006; Galban *et al*, 2008). However, it is not clear whether CPEB2-hindered HIF-1α synthesis occurs at elongation and thus secure a portion of HIF-1α RNA being polysome-associated. To detect HIF-1α in HeLa cells, the proteasome inhibitor MG132 was used to block degradation. The accumulation of HIF-1α was more sensitive to low concentrations of CHX than high concentrations of 4EGI-1 when compared with c-Myc, supporting that the rate-limiting step of HIF-1α RNA translation is at elongation (Figure 6A). The cells were then transfected with a plasmid expressing full-length (myc–CPEB2a) or eEF2-interacting mutants, the RNA-binding domain (myc–CPEB2C) or myc–CPEB2a Δ188–364, to monitor HIF-1α expression in the presence of MG132 (Figure 6B). The interaction of eEF2 with these CPEB2a mutants and CPEB2b was determined by co-IP (Supplementary Figure S5A). The lack of change in HIF-1α RNA levels showed that expression of CPEB2a, but not CPEB2a mutants, translationally downregulated HIF-1α synthesis (Figure 6C). This was also the case when CPEB2b was overexpressed (Supplementary Figure S5B and C). Overexpression of myc–CPEB2a did not affect global translation as judged by the polysome profiles (Figure 6D, left graphs). Interestingly, the repression of HIF-1α synthesis by wild-type, but not by mutant CPEB2 was accompanied by polysomal accumulation of HIF-1α RNA, showing that CPEB2–eEF2 interaction is required to constrain the rate-limiting step of HIF-1α translation at elongation (Figure 6D). The distribution of control GAPDH RNA was not affected by CPEB2 (Figure 6D).

To monitor whether the rate of *de-novo* HIF-1α synthesis is affected by CPEB2, HeLa cells with or without myc–CPEB2a expression were metabolically labelled with azidohomoalanine (AHA), a surrogate for methionine. The azide group in this modified amino acid could be conjugated with biotin-alkyne in a Click reaction, which allows the subsequent isolation of newly synthesized proteins using streptavidin beads (Dieterich *et al*, 2006). Unfortunately, we were unable to detect *de-novo* synthesized HIF-1α protein in the presence of MG132. We have also tried arsenite and $CoCl_2$ treatments and found that $CoCl_2$ robustly induced HIF-1α expression as reported in the previous study (Galban *et al*, 2008). The total and newly translated HIF-1α and c-Myc proteins were visualized by immunoblotting. The expression of HIF-1α but not c-Myc was inhibited by CPEB2 (Supplementary Figure S6A). To overcome the degradation problem and to determine whether CPEB2 affects translation of HIF-1α RNA through 3′-UTR, the EGFP reporter was appended with HIF-1α 3′-UTR

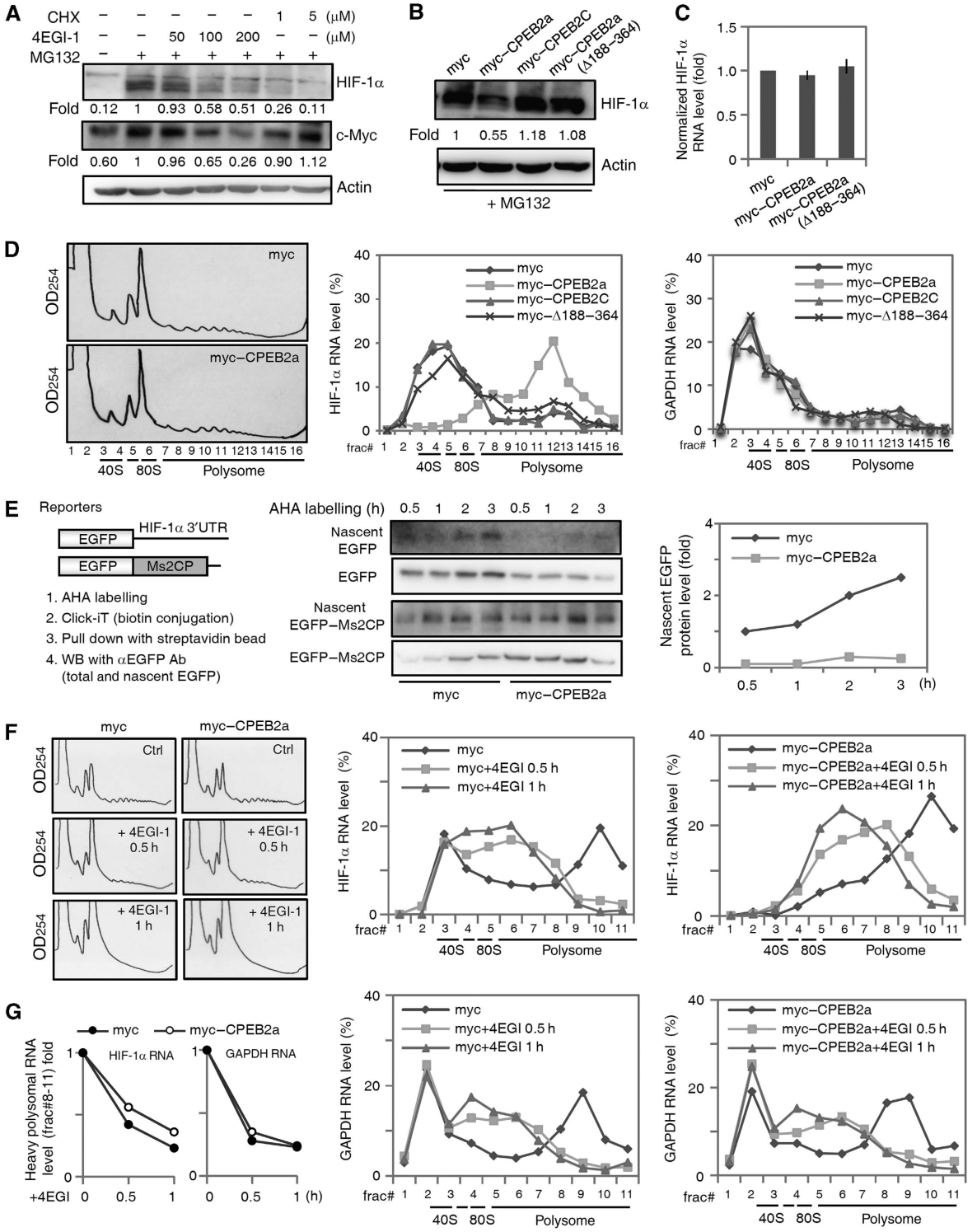

Figure 6 CPEB2 downregulates HIF-1α RNA translation. (**A**) Western blot analysis of HIF-1α–c-Myc, and actin using lysates from HeLa cells treated with ± 20 μM of MG132 and the indicated concentrations of CHX or 4EGI-1. The signals of HIF-1α and c-Myc were quantified and displayed as relative ratios (fold). (**B**) HeLa cells overexpressing myc–CPEB2a or its eEF2 binding-defective mutants (myc–CPEB2C and Δ188–364) were treated with 20 μM MG132 for 4 h and then used for western blotting (see also Supplementary Figure S5 for the interaction with eEF2), or (**C**) RNA isolation for quantitative RT–PCR (normalized with the GAPDH RNA level). (**D**) Two representative polysome profiles from HeLa cells with or without myc–CPEB2a expression. The polysomal distribution of HIF-1α and GAPDH RNAs in HeLa cells expressing myc, myc–CPEB2a, myc–CPEB2C, or the Δ188–364 mutant was determined by quantitative RT–PCR using RNAs isolated from each fraction. (**E**) HeLa cells transfected with plasmids encoding the two EGFP reporters with or without the HIF-1α 3′-UTR along with myc or myc–CPEB2a plasmid were metabolically labelled with AHA to tag *de-novo* synthesized polypeptides. EGFP and EGFP–Ms2CP from total cell lysate and the streptavidin-precipitated AHA-labelled proteins were detected by western blotting using EGFP Ab. The newly translated EGFP signals were quantified, expressed as a relative ratio and plotted against the time. (**F**) The polysome profiles of HeLa cells with or without myc–CPEB2a expression and ± 200 μM 4EGI-1 treatment. The polysomal distribution of HIF-1α and GAPDH RNA was determined by quantitative RT–PCR. (**G**) The amounts of HIF-1α and GAPDH RNAs in the heavy density polysome fractions (#8–11) in (**F**) were summed and plotted against the treatment time of 4EGI-1. The levels of HIF-1α and GAPDH RNAs at time zero were arbitrarily set to 1. Figure source data can be found in Supplementary data.

and the EGFP–Ms2CP was served as a non-target control. HeLa cells expressing the two EGFP reporters along with myc or myc–CPEB2a were labelled with AHA. EGFP and EGFP–Ms2CP from total cell lysate and the AHA-labelled proteins were detected by western blotting (Figure 6E). The synthesis of EGFP but not EGFP–Ms2CP was markedly suppressed by CPEB2 (Figure 6E). Since we could not detect *de-novo* synthesized HIF-1α protein even when degradation was blocked by MG132, the elongation rate (i.e., ribosome transit time, the time required for the ribosome to traverse the RNA) of HIF-1α synthesis was not experimentally measurable with the previously established method (Palmiter, 1972). To determine whether the elongation rate of HIF-1α RNA was hindered by CPEB2 with an alternative approach, we monitored the disappearance (ribosome unloading) of polysomal HIF-1α RNA in the presence of 4EGI-1 to prevent new initiation events (i.e., ribosome loading). Since the rate-limiting step in most RNA translations is at initiation, there is a remarkable reduction of the polysome size soon after 30 min treatment of 4EGI-1 (Figure 6F, left graphs). The amounts of HIF-1α and GAPDH RNAs from the heavy density polysomal fractions (#8–11) were calculated and plotted against the incubation time of 4EGI-1 (Figure 6G). Thus, the relative ribosome transit time of HIF-1α and GAPDH RNAs could be approximately compared with or without myc–CPEB2 expression. As expected, overexpression of CPEB2 has more effect on impeding the elongation of HIF-1α RNA than GAPDH RNA as assessed by the slower reduction of HIF-1α RNA in the heavy polysomal fractions (Figure 6G). It is worth noting that a deceleration at the termination step of HIF-1α RNA translation could also give rise the same result. Nevertheless, because CPEB2-repressed target RNA translation requires its interaction with eEF2 (Figures 5 and 6B), which has not been reported with a role at termination, such a slowdown in HIF-1α RNA translation most likely occurs at elongation.

If translation of HIF-1α RNA is retarded rather than paused by CPEB2, the accrued HIF-1α RNA at polysomes should be sensitive to puromycin treatment because puromycin resembles the aminoacylated tRNA and is only incorporated into translating ribosomes, not arrested ribosomes causing premature peptide chain and RNA release. Thus, the polysomal HIF-1α RNA would migrate towards lighter density fractions after the puromycin-induced release. Using HeLa cells, the distributions of HIF-1α and GAPDH RNAs after puromycin treatment were found to have moved towards lighter density fractions, even under CPEB2 overexpression (Supplementary Figure S6B). Together with the results from the GTP hydrolysis and reporter assays, CPEB2 slowed down but did not stop ribosomes from transiting along HIF-1α RNA, thereby permitting protein synthesis at a reduced rate.

Arsenite induces the dissociation of CPEB2 from HIF-1α RNA

To examine HIF-1α synthesis under CPEB2 KD conditions, we used Neuro-2a cells in which CPEB2 levels were high and more HIF-1α and polysome-associated HIF-1α RNA were detected. Thus, the influence of CPEB2 depletion on HIF-1α expression could be measured. In the CPEB2 KD cells, the level of HIF-1α protein, but not RNA, was elevated about 2.2-fold (Figure 7A and B), which correlated with a shift of HIF-1α but not GAPDH RNA, towards heavier density fractions. This revealed an enhanced association between HIF-1α mRNA and larger polysomes (Figure 7C). A great caution should be taken when interpreting the polysome data. The distribution of RNA shifted towards polysomes is generally considered to be translationally upregulated since the rate-limiting step of most RNA translation is at initiation. Nevertheless, the polysome profile by itself, simply reflects the number of ribosomes associated with the RNA that cannot be unequivocally equivalent to the translational status of the RNA (Mathews *et al*, 2007). For example, the change of HIF-1α RNA distribution in CPEB2 KD cells (Figure 7C) is either because initiation is stimulated or elongation/termination is inhibited, or both initiation and elongation are simultaneously stimulated or inhibited but with different magnitudes (i.e., an increase in initiation rate is greater than that in elongation rate, vice versa). Since CPEB2 slows down translation elongation of HIF-1α RNA, the depletion of CPEB2 is expected to accelerate the unloading of ribosomes from HIF-1α RNA, resulting in migration of HIF-1α RNA towards lighter density fractions if the regulation of HIF-1α RNA translation occurs only at elongation. That is not the case, so it appears that an unidentified mechanism that facilitates the ribosome loading (initiation events) on HIF-1α RNA is also enhanced in the KD cells. Notably, arsenite-induced HIF-1α synthesis was not evident in the KD cells and the amount of CPEB2 was not affected by arsenite. Similar situation was also found when cells were incubated in the 1% O_2 hypoxic chamber (Supplementary Figure S7A). Thus, we next examined whether arsenite reduced the CPEB2–HIF-1α RNA association by RNA-IP. Using non-specific GAPDH as a normalized control, there was more HIF-1α but not HIF-1β (non-target control) RNA in the CPEB2-containing precipitates isolated from mock-treated but not arsenite-treated cells (Figure 7D). Additionally, the reporter assay using the firefly luciferase appended with HIF-1α 3′-UTR showed that CPEB2 inhibited reporter RNA translation, which was no longer apparent in response to arsenite treatment (Figure 7E). This is also the case when the translation of reporter RNA is driven by CrPV IRES in an eIF-independent manner (Figure 7E). Using deletion mutant analysis, a non-canonical CPE-like sequence (UUUUCAU) in the 3′-UTR of HIF-1α RNA was required for CPEB2-mediated repression (Supplementary Figure S7B). RNA-IP of ectopically expressed myc–CPEB2a demonstrated that HIF-1α, but not GAPDH RNA, was also enriched in the myc–CPEB2a pull down from mock-treated rather than arsenite-treated cells (Figure 7F). Taken together, our results indicate that arsenite-increased HIF-1α synthesis is likely caused by the release of CPEB2 from HIF-1α RNA, which in turn alleviates CPEB2's inhibitory effect on eEF2 and enhances the elongation rate of HIF-1α RNA translation (Figure 7G).

Discussion

We have identified the molecular mechanism of CPEB2-repressed translation. Despite its functional resemblance with its family member CPEB1, CPEB2 uses a distinct mechanism to govern translation at elongation. The translocases, eEF2 in eukaryotes and EF-G in bacteria, are organized into two structural blocks: an N-terminal region containing domains I, G′, and II and a C-terminal region consisting of domains III, IV, and V. Although the mechanistic details of eEF2-catalysed GTP hydrolysis on the ribosome

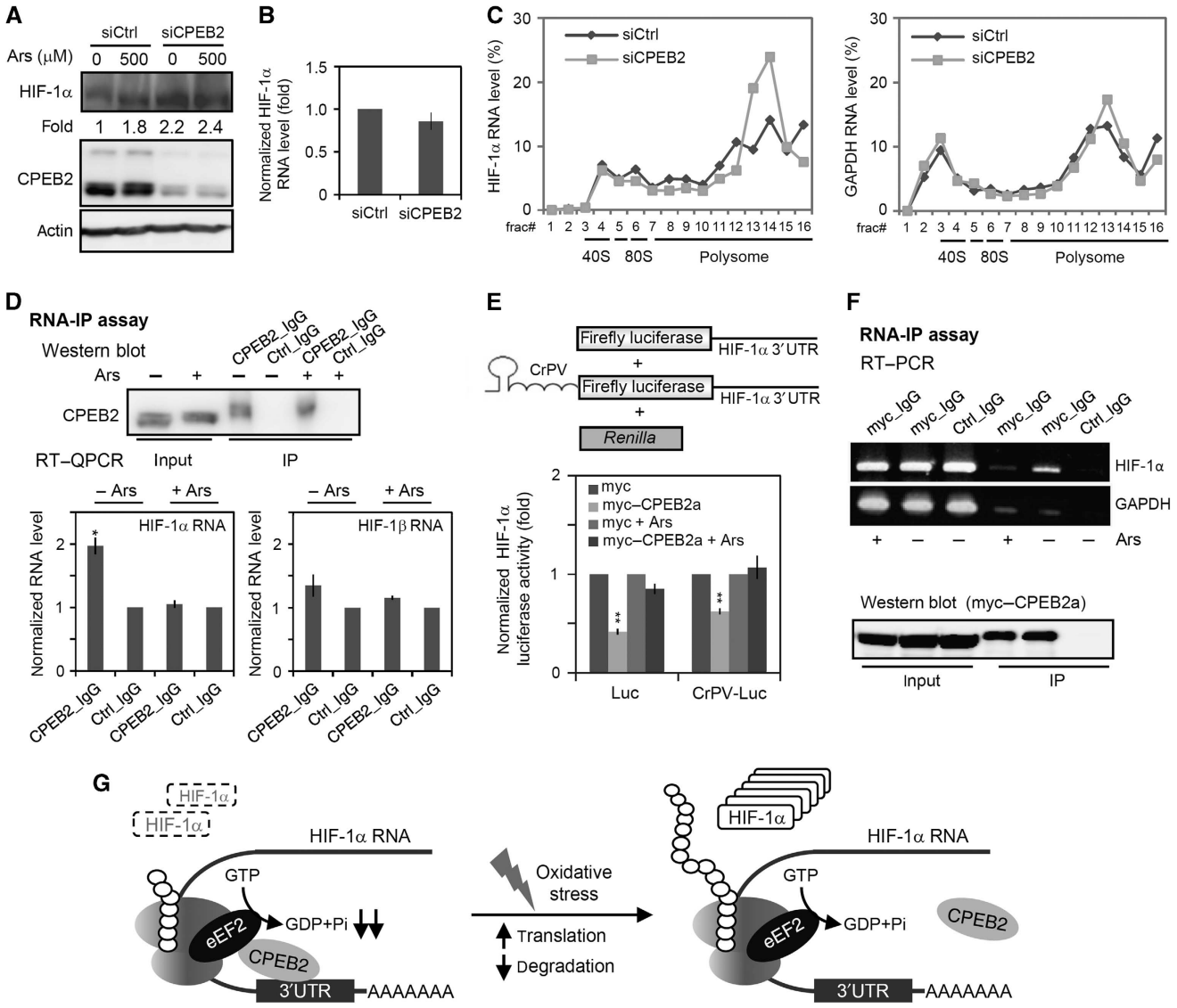

Figure 7 Arsenite reduces CPEB2–HIF-1α RNA association and elevates HIF-1α synthesis. (**A**) The siCtrl and siCPEB2 Neuro-2a cells were treated with or without arsenite for 30 min before detection of HIF-1α protein or (**B**) RNA levels (normalized with the GAPDH RNA level). (**C**) Polysomal distribution of HIF-1α and GAPDH RNAs in siCtrl and siCPEB2 Neuro-2a cells. (**D**) Neuro-2a cells treated with ± 500 μM arsenite for 30 min were used for RNA immunoprecipitation (RNA-IP). The control and CPEB2 IgG-precipitated substances were analysed for HIF-1α and HIF-1β RNAs by quantitative RT–PCR (normalized with the non-specific bound GAPDH RNA level). (**E**) The 293T cells transfected with the firefly luciferase reporter containing HIF-1α 3′-UTR ± CrPV IRES and *Renilla* luciferase along with myc or myc–CPEB2a were treated with ± 500 μM arsenite for 1 h and harvested for luciferase assay (normalized: firefly/*Renilla*) or (**F**) RNA-IP with myc Ab. The precipitated HIF-1α and GAPDH RNAs were analysed by RT–PCR. Error bars indicate s.e.m. ($n = 3$). One and two asterisks denote significant difference, $P < 0.05$ and $P < 0.01$, respectively (Student's *t*-test). (**G**) Schematic model of CPEB2-governed HIF-1α synthesis. In the well-oxygenated environment, the binding of CPEB2 to HIF-1α 3′-UTR reduces the HIF-1α peptide elongation through its interaction with eEF2. Arsenite-induced HIF-1α RNA translation is in part caused by the release of CPEB2 from HIF-1α RNA, which presumably allows eEF2 to resume its maximal GTPase activity and enhances translation elongation of HIF-1α RNA. Figure source data can be found in Supplementary data.

have not yet been unravelled at atomic resolution, cryo-EM reconstructions and X-ray structures of eEF2, EF-G, as well as the EF-G/70S ribosome complex indicate that the eEF2/EF-G molecule undergoes dynamic conformational changes to complete one round of GTP hydrolysis-dependent translocation in the course of its interaction with the ribosome (Jorgensen *et al*, 2003; Gao *et al*, 2009). Although the C-terminus of eEF2 is not directly in contact with GTP, binding of antibiotic inhibitors, such as fusidic acid or sordarin, in this region induces large-scale conformational changes of eEF2 that inhibits its function (Jorgensen *et al*, 2003; Soe *et al*, 2007). Because domain V of eEF2 is not required for ribosome docking and the CPEB2–eEF2–ribosome ternary complex could be detected *in vitro*, the binding of CPEB2 to domain V of eEF2 is likely to create steric hindrance that somehow interferes with the conformational changes of eEF2 on ribosomes, thereby affecting the efficiency of eEF2-mediated GTP hydrolysis. It is worth noting that our results did not completely exclude the possibility that eEF2 when in complex with CPEB2 might reduce its on-rate of binding to ribosomes and hence decreased its GTPase activity. Intriguingly, even though this inhibition could be reconstituted *in vitro* when CPEB2 was present at an equivalent or excess concentration to eEF2, CPEB2 did not affect

global translation *in vivo* even when overexpressed. Because the level of eEF2 is estimated to be about 100-fold higher than CPEB2 in Neuro-2a cells according to our western blot analysis, it is not surprising that CPEB2 slows down translation elongation only when bound to its target RNA. Two novel CPEB2 transcripts that encode the prevalent forms of CPEB2 in most tissues were identified from our study. However, all CPEB2 isoforms contain the eEF2-interacting motif and are capable of repressing translation. The functional entity, if any, carried by the uniquely spliced regions of the various isoforms will require further characterization.

CPEB-repressed translation: initiation versus elongation

A previous study showed that ectopically expressed CPEB1 but not CPEBs2–4 in oocytes pulled down the cleavage and polyadenylation specificity factor (CPSF) complex (Huang *et al*, 2006). In this study, we have identified that CPEBs2–3 employ a distinct mechanism to repress translation at elongation. Thus, CPEB1-mediated polyadenylation-induced translation initiation (Richter, 2007), that is, the elongated poly(A) tails of RNAs are bound by more poly(A)-binding proteins, which subsequently recruit eIF4G to compete with maskin for the binding to eIF4E, is unlikely to be a mechanism to alleviate CPEB2-repressed translation. To examine whether arsenite-induced HIF-1α synthesis requires polyadenylation of HIF-1α RNA, we performed the polyadenylation test assay (Salles *et al*, 1999). The poly(A) length of HIF-1α RNA remained unchanged under the arsenite treatment or overexpression of myc–CPEB1 or myc–CPEB2 (Supplementary Figure S8A). Both CPEB1- and CPEB2-mediated repression of the reporter RNAs were alleviated by arsenite without the need of polyadenylation signal, implying that polyadenylation is not a mechanism to increase HIF-1α RNA translation (Supplementary Figure S8B). This polyadenylation-independent mechanism was also employed by CPEB3 in neurons stimulated with *N*-methyl-D-aspartate (Huang *et al*, 2006). Further investigation is needed to understand how different extracellular cues lessen CPEB2- and CPEB3-mediated repression.

Translational control at elongation

Translation elongation is often considered to be regulated in a global manner through the reversible phosphorylation of eEF2 at Thr-56, which affects eEF2 binding to GTP (Carlberg *et al*, 1990; Nygard *et al*, 1991). Recently, eIF5A was identified to promote global translation elongation in yeasts and mammals (Saini *et al*, 2009; Li *et al*, 2010); while the other study showed that eIF5A was required mainly for efficient initiation and only facilitated elongation at the formation of the first peptide bond (Henderson and Hershey, 2011). In addition, translation elongation of RNAs encoding secretory or membrane proteins was delayed by the signal recognition particle (SRP) complex to preclude eEF2 docking on ribosomes (Mason *et al*, 2000; Halic *et al*, 2004; Mary *et al*, 2010). This elongation arrest provides sufficient time for binding of the SRP-paused nascent chain–ribosome complex to a limited number of SRP receptors on the endoplasmic reticulum (ER). Once translocation of the nascent signal peptide into ER is completed, removal of the SRP complex enables resumption of peptide elongation (Mason *et al*, 2000; Lakkaraju *et al*, 2008). Given the relative energy costs, elongation is not generally considered to be a highly regulated step in individual RNA translation; however, growing evidence suggests otherwise. For example, translation of Hac1 and Ash1 RNA in yeast was repressed at elongation through unique RNA sequence elements that form a loop or stem-loop structure, thereby stalling or attenuating, respectively, the movement of the ribosome along the RNA (Ruegsegger *et al*, 2001; Chartrand *et al*, 2002). In mammals, the C-terminal 26 amino acids of XBP1u were recently shown to halt its peptide elongation through an unidentified mechanism (Yanagitani *et al*, 2011). TGF-β-activated epithelial–mesenchymal transition (EMT) requires translational induction of disabled-2 and interleukin-like EMT inducer. This translational control in the epithelial state is mediated by hnRNP E1 to block eEF1A1 release from the ribosome and stall translation at elongation (Hussey *et al*, 2011). In response to TGF-β signalling, the phosphorylation of hnRNP E1 results in its dissociation from the 3′-UTRs of EMT transcripts, hence peptide elongation is resumed (Chaudhury *et al*, 2010). Besides hnRNP E1, CPEB2 is another RNA-binding protein identified to control elongation of selective transcripts via a distinct mechanism.

Elongation control: to stop or to slow down

Slowing down translation of HIF-1α RNA by CPEB2 under normoxia has two obvious advantages. First, it produces less HIF-1α to be degraded and hence preserves cellular energy and reduces the loading of proteasomes. Second, such control seems to be necessary to impose the rate-limiting step of HIF-1α translation at elongation that ensures a portion of HIF-1α RNA being ribosome-associated and ready for the first few rounds of prompt syntheses in response to hypoxia. Then, why does translation of HIF-1α RNA prefer to slow rather than pause elongation with a higher cost of energy expenditure? Perhaps, an even faster production of HIF-1α by removing the elongation repressor CPEB2 at the beginning of hypoxia is needed to achieve maximal survival of cells since global protein synthesis is significantly downregulated through phosphorylation of several translation factors, such as eIF-2α, 4E-BP1, and eEF2, soon after cells are exposed to such a stressful environment (Connolly *et al*, 2006; Yee Koh *et al*, 2008; Majmundar *et al*, 2010). Other RNA-binding proteins, such as HuR and polypyrimidine tract-binding protein, bind to HIF-1α RNA and sustain its protein production under hypoxia-decreased global translation condition (Galban *et al*, 2008). Thus, translation of HIF-1α RNA is regulated by an array of RNA-binding proteins. Moreover, CPEB2 is not ubiquitously expressed and HIF-1α levels vary between cells; therefore, CPEB2-controlled HIF-1α RNA translation could be important for some tissues and not others. It will be of great interest to identify other RNAs that are subject to CPEB2-mediated translational control. In summary, our study reveals a unique example of how the elongation rate of translation can be modulated in a target-specific manner through a *trans*-acting RNA-binding protein.

Materials and methods

Antibodies and chemicals

Antibodies used in the study were eEF2 (cat #13004), HIF-1α (cat #10790), c-Myc (cat #764), and RPS6 (cat #74576) from Santa Cruz Biotechnology; EGFP (cat #G1544), β-actin (cat #A5441), and flag epitope (cat #F1804) form Sigma-Aldrich. The anti-CPEB2 serum was raised using the N-terminal 261 a.a. of mCPEB2 (NP_787951)

produced in *E. coli*. Except 4EGI-1 (cat #202597) was from Santa Cruz Biotechnology, all other chemicals were from Sigma-Aldrich.

Identification of CPEB2a/b transcripts and plasmid construction

Using primers designed according to the predicted clone (XM_0010602399, 724 a.a.), 5′-gaagatctaccATGCGGGACTTCGGGT TC-3′ and 5′-acgtcgacTTAGTTCCAGCGGAAGTGG-3′, two isoforms, CPEB2a and CPEB2b, were amplified from rat hippocampal neuron cDNA. The CPEB2a and CPEB2b isoforms were cloned into the pcDNA3.1-myc plasmid. The various lengths of eEF2 were PCR amplified from mouse brain cDNA and cloned into the pGADT7 or pcDNA3.1-flag plasmid. The N-terminal 456 and 486 a.a. of CPEB2a and CPEB2b, respectively, were cloned to pGBK-T7 for yeast two-hybrid interaction or fused to the dimeric Ms2CP for the reporter assay (Huang *et al*, 2006). The hp/CrPV IRES sequence was PCR amplified from the php/CrPV/R-Gl plasmid (Isken *et al*, 2008), and cloned as the 5′-UTR of firefly luciferase reporter with two Ms2CP-binding sites appended at the 3′-UTR (Huang *et al*, 2006). The 3′-UTR of HIF-1α RNA was amplified from rat brain cDNA and cloned into the reporter construct. The deletion mutants of myc–CPEB2aN–Ms2CP, myc–CPEB3aN–Ms2CP, and HIF-1α 3′-UTR were generated by QuikChange Site-Directed Mutagenesis Kit (Stratagene) according to the manufacturer's protocol.

Yeast two-hybrid screen

The procedures using the random-primed mouse brain library were described previously (Peng *et al*, 2010), except using the rCPEB2a N-terminus as the bait.

Cell culture, lentivirus infection, and transfection

Cultures of rat hippocampal and cortical neurons and infections of neurons with lentiviral particles expressing control or shRNA against CPEB2 were as previously described (Peng *et al*, 2010). HEK-293T, HeLa, and Neuro-2a cells were cultured in DMEM with 10% FBS. Transfection of plasmid DNAs was carried out using lipofectamine 2000 (Invitrogen) following the manufacturer's protocol.

Co-IP and RNA-IP

For co-IP, the transfected 293T cells were lysed in IP buffer (50 mM Hepes, pH 7.4, 150 mM NaCl, 1 mM $MgCl_2$, 0.5% Triton X-100, 10% glycerol, 1 mM DTT, 1 × protease inhibitor cocktail, and 200 μg/ml RNase A) and centrifuged at 10 000 *g* for 3 min. The supernatants were incubated with protein G beads bound with myc or flag Ab. The beads were washed three times with IP buffer and the precipitated proteins were used for western blotting. For reciprocal IP of endogenous CPEB2 and eEF2, Neuro-2a cells were lysed in IP buffer with or without 200 μg/ml RNase A and centrifuged at 10 000 *g* for 3 min. Equal volumes of supernatant were incubated with eEF2, CPEB2, or control IgG-bound beads and the precipitated substances were immunoblotted with CPEB2 and eEF2 Abs. Similarly to reciprocal IP except the Neuro-2a or transfected 293T cells were lysed in IP buffer without RNase A for RNA-IP and the immunoprecipitates were eluted with the buffer (100 mM Tris, pH 8, 10 mM EDTA, and 1% SDS), phenol/chloroform extracted and ethanol precipitated to isolate RNA.

80S ribosome, eEF2, and recombinant protein purification

The 80S ribosome from *Artemia salina* cysts and eEF2 from rat livers were isolated according to the published protocols with modifications (Iwasaki and Kaziro, 1979). A rat liver was homogenized in 20 ml buffer (20 mM Tris, pH 7.6, 6 mM $MgCl_2$, 0.25 M sucrose, 10 mM β-mercaptoethanol, and 1 mM PMSF) and the clear supernatant after three spins at 15 000 *g* for 10 min was made 30% (w/v) in ammonium sulphate under stirring for 1 h at 4 °C. The precipitated proteins harvested by centrifugation at 10 000 *g* for 10 min were dissolved in 10 ml of dialysis buffer (20 mM Tris–HCl, pH 8.0, 50 mM KCl, 0.1 mM EDTA, 10% glycerol, 10 mM β-mercaptoethanol, and 1 mM PMSF) and dialysed against the same buffer. The dialysed material was filtered through a 0.2-μm PVDF filter and the clear filtrate was applied to Mono Q column (GE Healthcare). The eluted fractions containing eEF2 were collected (∼2 ml), diluted with 8 ml of 20 mM Tris–HCl, pH 6.8 and subsequently purified by Mono S column (GE Healthcare). The eluted eEF2 was dialysed against the GTPase assay buffer (20 mM Tris, pH 8, 100 mM KCl, 5 mM $MgCl_2$, 10% glycerol, and 10 mM β-mercaptoethanol), aliquoted and stored at −80°C. To increase the solubility of CPEB2, CPEB2a as well as the control, EGFP–Ms2CP was cloned to pE-sumo plasmid (Marblestone *et al*, 2006). The transformed BL21 star (DE3) *E. coli* (Invitrogen) were grown to a measured A_{600} of 0.5 and induced with 0.4 mM IPTG for 16 h at 23°C. The pelleted bacteria were lysed and sonicated in the buffer (50 mM Tris–HCl, pH 8, 500 mM NaCl, 0.2% Triton X-100, 10% glycerol, 10 mM imidazole, 1 mg/ml lysozyme, 10 mM β-mercaptoethanol, and 1 mM PMSF), followed by an affinity purification using Ni-NTA resin (Qiagen). The imidazole-eluted proteins were dialysed in the GTPase buffer and concentrated using Spin-X concentrators (Corning).

GTPase assay and ribosome co-IP

The eEF2/ribosome-promoted GTP hydrolysis was assessed using thin layer chromatography (Yeh *et al*, 2007). Unless specified, reactions typically containing 0.5 pmol eEF2, 0.5 pmol recombinant protein (EGFP–Ms2CP or CPEB2a), 0.3 pmol 80S ribosome and 2 nmol GTP (containing 0.5 μCi γ^{32}P-GTP) in 10 μl GTPase assay buffer, were incubated at 37°C for the indicated time and then stopped by 20 mM EDTA. One microlitre aliquot from each reaction was spotted onto polyethyleneimine-cellulose plate (Sigma-Aldrich) and chromatographed with 0.5 M LiCl and 1 M formic acid. The radioactive signals were analysed and quantified by phosphoimager. To test whether CPEB2 binds to eEF2 situated on ribosomes, the reactions after 30 min incubation were immunoprecipitated with CPEB2 or control IgG. The beads were washed three times with GTPase assay buffer and eluted with the buffer (100 mM Tris, pH 8, 10 mM EDTA, and 1% SDS), followed by phenol/chloroform extraction and ethanol precipitation with 20 μg yeast tRNA as a carrier. The precipitated RNAs were used for RT–PCR using primers for *A. salina* ribosomal RNAs: 18S, 5′-CATGGCAAGGTGGCCTACTC-3′ and 5′-GCAACCATGGTAGGCGCATA-3′; 28S, 5′-GATGAGAAGACCGAT GGCGG-3′ and 5′-TCCTTGCCGCTAACAACACC-3′.

RNA extraction, cDNA synthesis, and quantitative PCR

Sucrose gradient fractions were treated with 100 μg/ml Proteinase K and 0.2% SDS for 30 min at 37°C, phenol/chloroform extracted and precipitated with isopropanol to obtain RNAs. The other procedures were described previously (Peng *et al*, 2010) except the primers used for quantitative PCR (QPCR) are hHIF-1α, 5′-tttttcaagcagtaggaattg ga-3′ and 5′-gtgatgtagtagctgcatgatcg-3′; mHIF-1α, 5′-gcactagacaaagtt cacctgaga-3′ and 5′-cgctatccacatcaaagcaa-3′; hGAPDH, 5′-agccacatc\ gctcagacac-3′ and 5′-gcccaatacgaccaaatcc-3′; mGAPDH, 5′-gccaaaag ggtcatcatctc-3′ and 5′-cacacccatcacaaacatgg-3′; mHIF-1β, 5′-TGCCT CATCTGGTACTGCTG-3′ and 5′-TGTCCTGTGGTCTGTCCAGT-3′.

Luciferase reporter assay

A mixture of plasmid DNAs containing 0.62 μg Ms2CP fusions, 0.15 μg firefly luciferase, and 0.03 μg *Renilla* luciferase reporters were co-transfected into 293T cells. Cells were treated with or without 2 μM cycloheximide or 100 μM 4EGI-1 at 6 h after transfection and harvested after 12 h. The protein lysates were analysed using Dual-Luciferase Reporter Assay System (Promega).

Sucrose density gradient for polysomal profiling

Depending on the experiments, the global translation status of cells harvested for polysome study varied depending on the confluence and culture condition of cells. Nonetheless, all polysome experiments were performed 2–3 times independently to derive the conclusion. For the overexpression experiment (Figure 6D), the HeLa cells were subcultured on the day before transfection and harvested ∼24 h later without change of fresh medium. For the ribosome transit time study (Figure 6F), the overday transfected 15 cm dish of HeLa cells were subcultured into three 10 cm dishes and incubated overnight prior to 4EGI-1 treatment. For the KD experiment (Figure 7C), Neuro-2a cells were subcultured 2 days after transfection and harvested ∼20 h later. HeLa or Neuro-2a cells were washed once with PBS, lysed in polysome buffer (25 mM Hepes, pH 7.5, 25 mM NaCl, 5 mM $MgCl_2$, 0.3% NP-40, 100 μg/ml cycloheximide, 0.5 mM DTT, 20 U/ml RNase inhibitor and 1 × protease inhibitor cocktail) and centrifuged at 10 000 *g* for 5 min at 4°C. In all, 20 μl of supernatant was used for total RNA isolation and the other 200 μl was layered on top of a linear 15–50% (w/v) sucrose gradient. Centrifugation was carried out in an SW41 rotor at 37 000 r.p.m. for 2 h. Polysome profiles were monitored by absorbance of 254 nm light using ISCO density gradient system.

Proteins of gradient fractions were precipitated using 0.1 μg/ml deoxycholate and 10% trichloroacetic acid and used for western blotting.

Click-iT assay

The overnight transfected 6 cm dish of HeLa cells was replaced with methionine-free medium with or without 500 μM $CoCl_2$. After 30 min incubation, the Click-iT AHA (L-azidohomoalanine) was added to a final concentration of 50 μM to metabolically label nascent synthesized polypeptides. The labelled cells were harvested and lysed in IP buffer without DTT. The protein concentration was determined by BCA protein assay (Pierce) and 100 μg protein from each lysate was conjugated with biotin-alkyne according to the manufacturer's protocol (Invitrogen). The *de-novo* translated proteins were precipitated with Dynabeads M-280 Streptavidin (Invitrogen) and analysed by western blotting.

Accession number

The nucleotide and protein sequences of CPEB2a and CPEB2b were deposited in the NCBI database, JF973322 and JF973323.

Supplementary data

Supplementary data are available at *The EMBO Journal* Online (http://www.embojournal.org).

Acknowledgements

We thank Lynne Maquat for the php/CrPV/R-Gl plasmid and David Chuang for the pE-Sumo plasmid. We appreciate Teng-Nan Lin for sharing the hypoxic chamber device. This work was supported by grants from the National Science Council (NSC 99-2311-B-001-020-MY3), National Health Research Institute (NHRI-EX100-9814NI), and Academia Sinica (AS-100-TP-B09) in Taiwan.

Author contributions: P-JC performed all experiments except the cloning of CPEB2a and CPEB2b sequences and the purification of eEF2, which were conducted by Y-SH. Y-SH supervised the study and wrote the manuscript with the contribution from P-JC.

Conflict of interest

The authors declare that they have no conflict of interest.

References

Carlberg U, Nilsson A, Nygard O (1990) Functional properties of phosphorylated elongation factor 2. *Eur J Biochem* **191:** 639–645

Chartrand P, Meng XH, Huttelmaier S, Donato D, Singer RH (2002) Asymmetric sorting of ash1p in yeast results from inhibition of translation by localization elements in the mRNA. *Mol Cell* **10:** 1319–1330

Chaudhury A, Hussey GS, Ray PS, Jin G, Fox PL, Howe PH (2010) TGF-beta-mediated phosphorylation of hnRNP E1 induces EMT via transcript-selective translational induction of Dab2 and ILEI. *Nat Cell Biol* **12:** 286–293

Clark IE, Wyckoff D, Gavis ER (2000) Synthesis of the posterior determinant Nanos is spatially restricted by a novel cotranslational regulatory mechanism. *Curr Biol* **10:** 1311–1314

Connolly E, Braunstein S, Formenti S, Schneider RJ (2006) Hypoxia inhibits protein synthesis through a 4E-BP1 and elongation factor 2 kinase pathway controlled by mTOR and uncoupled in breast cancer cells. *Mol Cell Biol* **26:** 3955–3965

Dieterich DC, Link AJ, Graumann J, Tirrell DA, Schuman EM (2006) Selective identification of newly synthesized proteins in mammalian cells using bioorthogonal noncanonical amino acid tagging (BONCAT). *Proc Natl Acad Sci U S A* **103:** 9482–9487

Galban S, Kuwano Y, Pullmann Jr R, Martindale JL, Kim HH, Lal A, Abdelmohsen K, Yang X, Dang Y, Liu JO, Lewis SM, Holcik M, Gorospe M (2008) RNA-binding proteins HuR and PTB promote the translation of hypoxia-inducible factor 1alpha. *Mol Cell Biol* **28:** 93–107

Gao YG, Selmer M, Dunham CM, Weixlbaumer A, Kelley AC, Ramakrishnan V (2009) The structure of the ribosome with elongation factor G trapped in the posttranslocational state. *Science* **326:** 694–699

Hagele S, Kuhn U, Boning M, Katschinski DM (2009) Cytoplasmic polyadenylation-element-binding protein (CPEB)1 and 2 bind to the HIF-1alpha mRNA 3′-UTR and modulate HIF-1alpha protein expression. *Biochem J* **417:** 235–246

Halic M, Becker T, Pool MR, Spahn CM, Grassucci RA, Frank J, Beckmann R (2004) Structure of the signal recognition particle interacting with the elongation-arrested ribosome. *Nature* **427:** 808–814

Hartman H, Smith TF (2010) GTPases and the origin of the ribosome. *Biol Direct* **5:** 36

Henderson A, Hershey JW (2011) Eukaryotic translation initiation factor (eIF) 5A stimulates protein synthesis in Saccharomyces cerevisiae. *Proc Natl Acad Sci USA* **108:** 6415–6419

Herbert TP, Proud CG (2007) Regulation of translation elongation and the cotranslational protein targeting pathway. In: Mathews MB, Sonenberg N, Hershey JWB (eds). *Translational Control in Biology and Medicine*, vol. 21 **21**. Cold Spring Harbor Laboratory Press: Cold Spring Harbor, NY pp 601–624

Huang YS, Kan MC, Lin CL, Richter JD (2006) CPEB3 and CPEB4 in neurons: analysis of RNA-binding specificity and translational control of AMPA receptor GluR2 mRNA. *EMBO J* **25:** 4865–4876

Huang YS, Richter JD (2007) Analysis of mRNA translation in cultured hippocampal neurons. *Methods Enzymol* **431:** 143–162

Hui AS, Bauer AL, Striet JB, Schnell PO, Czyzyk-Krzeska MF (2006) Calcium signaling stimulates translation of HIF-alpha during hypoxia. *FASEB J* **20:** 466–475

Hussey GS, Chaudhury A, Dawson AE, Lindner DJ, Knudsen CR, Wilce MC, Merrick WC, Howe PH (2011) Identification of an mRNP complex regulating tumorigenesis at the translational elongation step. *Mol Cell* **41:** 419–431

Isken O, Kim YK, Hosoda N, Mayeur GL, Hershey JW, Maquat LE (2008) Upf1 phosphorylation triggers translational repression during nonsense-mediated mRNA decay. *Cell* **133:** 314–327

Iwasaki K, Kaziro Y (1979) Polypeptide chain elongation factors from pig liver. *Methods Enzymol* **60:** 657–676

Jorgensen R, Ortiz PA, Carr-Schmid A, Nissen P, Kinzy TG, Andersen GR (2003) Two crystal structures demonstrate large conformational changes in the eukaryotic ribosomal translocase. *Nat Struct Biol* **10:** 379–385

Jung MY, Lorenz L, Richter JD (2006) Translational control by neuroguidin, a eukaryotic initiation factor 4E and CPEB binding protein. *Mol Cell Biol* **26:** 4277–4287

Kan MC, Oruganty-Das A, Cooper-Morgan A, Jin G, Swanger SA, Bassell GJ, Florman H, van Leyen K, Richter JD (2010) CPEB4 is a cell survival protein retained in the nucleus upon ischemia or endoplasmic reticulum calcium depletion. *Mol Cell Biol* **30:** 5658–5671

Lakkaraju AK, Mary C, Scherrer A, Johnson AE, Strub K (2008) SRP keeps polypeptides translocation-competent by slowing translation to match limiting ER-targeting sites. *Cell* **133:** 440–451

Li CH, Ohn T, Ivanov P, Tisdale S, Anderson P (2010) eIF5A promotes translation elongation, polysome disassembly and stress granule assembly. *PLoS One* **5:** e9942

Lin CL, Evans V, Shen S, Xing Y, Richter JD (2010) The nuclear experience of CPEB: implications for RNA processing and translational control. *RNA* **16:** 338–348

Majmundar AJ, Wong WJ, Simon MC (2010) Hypoxia-inducible factors and the response to hypoxic stress. *Mol Cell* **40:** 294–309

Marblestone JG, Edavettal SC, Lim Y, Lim P, Zuo X, Butt TR (2006) Comparison of SUMO fusion technology with traditional gene fusion systems: enhanced expression and solubility with SUMO. *Protein Sci* **15:** 182–189

Mary C, Scherrer A, Huck L, Lakkaraju AK, Thomas Y, Johnson AE, Strub K (2010) Residues in SRP9/14 essential for elongation arrest activity of the signal recognition particle define a positively charged functional domain on one side of the protein. *RNA* **16:** 969–979

Mason N, Ciufo LF, Brown JD (2000) Elongation arrest is a physiologically important function of signal recognition particle. *EMBO J* **19:** 4164–4174

Mathews MB, Sonenberg N, Hershey JWB (2007) Origins and principles of translational control. In: Mathews MB, Sonenberg

N, Hershey JWB (eds). *Translational Control in Biology and Medicine*, vol. 1 Cold Spring Harbor Laboratory Press: Cold Spring Harbor, NY pp 1–40

Mendez R, Richter JD (2001) Translational control by CPEB: a means to the end. *Nat Rev Mol Cell Biol* **2:** 521–529

Merrick WC, Nyborg J (2000) The protein biosynthesis elongation cycle. In: Sonenberg N, Hershey JWB, Mathews MB (eds). *Translational Control of Gene Expression*. Cold Spring Harbor Laboratory Press: Cold Spring Harbor, NY pp 89–125

Moerke NJ, Aktas H, Chen H, Cantel S, Reibarkh MY, Fahmy A, Gross JD, Degterev A, Yuan J, Chorev M, Halperin JA, Wagner G (2007) Small-molecule inhibition of the interaction between the translation initiation factors eIF4E and eIF4G. *Cell* **128:** 257–267

Nygard O, Nilsson A, Carlberg U, Nilsson L, Amons R (1991) Phosphorylation regulates the activity of the eEF-2-specific Ca(2+)- and calmodulin-dependent protein kinase III. *J Biol Chem* **266:** 16425–16430

Olsen PH, Ambros V (1999) The lin-4 regulatory RNA controls developmental timing in Caenorhabditis elegans by blocking LIN-14 protein synthesis after the initiation of translation. *Dev Biol* **216:** 671–680

Palmiter RD (1972) Regulation of protein synthesis in chick oviduct. II. Modulation of polypeptide elongation and initiation rates by estrogen and progesterone. *J Biol Chem* **247:** 6770–6780

Peng SC, Lai YT, Huang HY, Huang HD, Huang YS (2010) A novel role of CPEB3 in regulating EGFR gene transcription via association with Stat5b in neurons. *Nucleic Acids Res* **38:** 7446–7457

Pestova TV, Hellen CU (2003) Translation elongation after assembly of ribosomes on the Cricket paralysis virus internal ribosomal entry site without initiation factors or initiator tRNA. *Genes Dev* **17:** 181–186

Pestova TV, Lorsch JR, Hellen CUT (2007) The mechanism of translation initiation in eukaryotes. In: Mathews MB, Sonenberg N, Hershey JWB (eds) *Translational Control in Biology and Medicine*, vol. 4 Cold Spring Harbor Laboratory Press: Cold Spring Harbor, NY pp 87–128

Richter JD (2007) CPEB: a life in translation. *Trends Biochem Sci* **32:** 279–285

Richter JD, Sonenberg N (2005) Regulation of cap-dependent translation by eIF4E inhibitory proteins. *Nature* **433:** 477–480

Ruegsegger U, Leber JH, Walter P (2001) Block of HAC1 mRNA translation by long-range base pairing is released by cytoplasmic splicing upon induction of the unfolded protein response. *Cell* **107:** 103–114

Saini P, Eyler DE, Green R, Dever TE (2009) Hypusine-containing protein eIF5A promotes translation elongation. *Nature* **459:** 118–121

Salles FJ, Richards WG, Strickland S (1999) Assaying the polyadenylation state of mRNAs. *Methods* **17:** 38–45

Soe R, Mosley RT, Justice M, Nielsen-Kahn J, Shastry M, Merrill AR, Andersen GR (2007) Sordarin derivatives induce a novel conformation of the yeast ribosome translocation factor eEF2. *J Biol Chem* **282:** 657–666

Sonenberg N, Hinnebusch AG (2009) Regulation of translation initiation in eukaryotes: mechanisms and biological targets. *Cell* **136:** 731–745

Stebbins-Boaz B, Cao Q, de Moor CH, Mendez R, Richter JD (1999) Maskin is a CPEB-associated factor that transiently interacts with elF-4E. *Mol Cell* **4:** 1017–1027

Theis M, Si K, Kandel ER (2003) Two previously undescribed members of the mouse CPEB family of genes and their inducible expression in the principal cell layers of the hippocampus. *Proc Natl Acad Sci USA* **100:** 9602–9607

Thomas JD, Johannes GJ (2007) Identification of mRNAs that continue to associate with polysomes during hypoxia. *RNA* **13:** 1116–1131

Waerner T, Alacakaptan M, Tamir I, Oberauer R, Gal A, Brabletz T, Schreiber M, Jechlinger M, Beug H (2006) ILEI: a cytokine essential for EMT, tumor formation, and late events in metastasis in epithelial cells. *Cancer Cell* **10:** 227–239

Wilson JE, Pestova TV, Hellen CU, Sarnow P (2000) Initiation of protein synthesis from the A site of the ribosome. *Cell* **102:** 511–520

Yanagitani K, Kimata Y, Kadokura H, Kohno K (2011) Translational Pausing Ensures Membrane Targeting and Cytoplasmic Splicing of XBP1u mRNA. *Science* **331:** 586–589

Yee Koh M, Spivak-Kroizman TR, Powis G (2008) HIF-1 regulation: not so easy come, easy go. *Trends Biochem Sci* **33:** 526–534

Yeh YH, Kesavulu MM, Li HM, Wu SZ, Sun YJ, Konozy EH, Hsiao CD (2007) Dimerization is important for the GTPase activity of chloroplast translocon components atToc33 and psToc159. *J Biol Chem* **282:** 13845–13853